Undetectable JPEG Image Batch Reversible Data Hiding with Content-adaptive Payload Allocation

Yangguang Wang, Jinwei Li, Yuanzhi Yao*, and Nenghai Yu
School of Information Science and Technology
University of Science and Technology of China, Hefei 230027, China
e-mail: wang2013@mail.ustc.edu.cn, ljwyyq@mail.ustc.edu.cn, yaoyz@ustc.edu.cn, ynh@ustc.edu.cn

***Abstract*—As an efficient way to achieve covert storage in clouds, batch image data hiding attracts increasing attention in recent years. Reversible data hiding which can completely restore the original covers after data extraction brings about novel advantages for JPEG image-based covert storage. However, due to the specific manipulation on DCT coefficients, existing JPEG image reversible data hiding cannot meet the requirement of secure covert storage. Therefore, the undetectability of batch JPEG image reversible data hiding deserves investigation. In this paper, we propose an undetectable JPEG image batch reversible data hiding method, in which a content-adaptive payload allocation strategy is designed to enhance the undetectability and guarantee the reversibility. Experimental results show the superiority of this proposed method compared with the state-of-the-art related methods.**

I. Introduction

Batch image data hiding which serves as an efficient way to achieve covert storage in clouds attracts increasing attention in recent years. Reversible data hiding (RDH) which can imperceptibly hide data into digital images and completely reconstruct the original image after data extraction [1]–[5] brings about novel advantages for image-based covert storage. Considering that the joint photographic experts group (JPEG) is the most popular format of digital images, most image-based applications focus on JPEG format.

Recently, JPEG image reversible data hiding has achieved good performance in the balance of distortion, embedding capacity, and file size expansion [6]–[11]. DCT coefficients are the main cover elements of JPEG image reversible data hiding, because DCT coefficients usually follow the sharp Laplacian distribution after DCT transformation and quantization. In 2016, Huang *et al.* [6] applied histogram shifting in JPEG image reversible data hiding, which aims to select appropriate DCT coefficients for modification. Besides, the block selection strategy is used to decide the embedding order for reducing embedding distortion. Hou *et al.* [9] made improvements on Huang *et al.*'s method [6] by considering the influence of quantization steps and simulated distortions in blocks before data embedding. The method [9] utilizes the selection strategy of DCT coefficients and image blocks, which can keep good rate-distortion performance and a small file size expansion. Yin *et al.* [11] proposed to use multi-objective optimization strategy to balance the distortion and file size expansion. Experimental results show that this method [11] outperforms the previous works in both rate-distortion and file size expansion.

As shown in [12], more than 4000 photos are uploaded per second on Facebook. This indicates that image-based covert storage on social platforms can provide considerable storage room. The advantage of applying JPEG image reversible data hiding in covert storage is that the original images can be losslessly recovered after data extraction. However, many state-of-the-art JPEG image reversible data hiding methods [6], [9], [11] mainly concentrate on embedding data in a single image and ignore how to allocate the to-be-embedded data in multiple images. The undetectability of JPEG image reversible data hiding [13] remains an unresolved problem and restrains the JPEG image-based covert storage applications. Therefore, undetectable JPEG image batch reversible data hiding deserves investigation.

To tackle the above unresolved problem, the undetectable JPEG image batch reversible data hiding method is proposed in this paper. Firstly, the texture complexity of each JPEG image is modeled to determine the embedding order for each cover image. Secondly, the content-adaptive payload allocation strategy is proposed to enhance the undetectability of JPEG image batch reversible data hiding. Thirdly, the synchronization mechanism is designed to guarantee the reversibility because the texture complexity may be modified after data embedding. The main contributions of this paper are summarized as follows.

- The texture complexity of each JPEG image is modeled to determine the embedding order for each cover image.
- The content-adaptive payload allocation strategy is designed to enhance the undetectability and guarantee the reversibility.
- Extensive experiments demonstrate the merits of the proposed undetectable JPEG image batch reversible data hiding method.

The remainder of this paper is organized as follows. Section II introduces the state-of-the-art JPEG image reversible data hiding methods. Section III presents our proposed method in detail followed by the experimental results in Section IV. Finally, Section V concludes this paper.

II. Related Works

Recently, some state-of-the-art histogram shifting-based reversible data hiding methods for single JPEG image strike a

*Corresponding author.

balance between visual distortion, file size expansion, and embedding capacity [6], [9], [11]. For convenience, the technical details of these methods [6], [9], [11] are elaborated as follows.

A. Huang et al.'s Method

Huang *et al.* [6] found that due to quantization, most of the nonzero DCT coefficients belonging to high frequencies have a value of ± 1 in general. As expected, the peak points of the nonzero AC coefficients histogram are generally located at bins ± 1, so it is taken for granted that the ± 1 AC coefficients can be expanded to carry secret data [14]. The embedding and extracting procedures are briefly reviewed below.

We define $b_i(u,v)$ where $u,v = 0,1,2,\cdots,7$ as a 8×8 block of the quantized DCT coefficients, and sort all b_i in descending order according to the number of zero AC coefficients in each b_i. Thus we can get $B = \{b_1, b_2, \cdots, b_N\}$, where N is the total number of all the 8×8 DCT blocks in a JPEG image.

Then, we embed data based on the sorted B. For example, $b_i(u,v)$, we scan the DCT coefficients of $b_i(u,v)$ in order, and the embedded data (d) and the revised $b_i'(u,v)$ can be calculated by

$$b_i' = \begin{cases} b_i + \text{sign}(b_i) \times d, & \text{if } |b_i| = 1 \\ b_i + \text{sign}(b_i), & \text{if } |b_i| > 1 \end{cases} \tag{1}$$

where b_i and b_i' are short for $b_i(u,v)$ and $b_i'(u,v)$, and sign$(\cdot)$ is the sign function defined by

$$\text{sign}(x) = \begin{cases} 1, & \text{if } x > 0 \\ 0, & \text{if } x = 0 \\ -1, & \text{if } x < 0. \end{cases} \tag{2}$$

During the extracting procedures, it is obvious that the original zero AC coefficients keep unchanged, and no new zero AC coefficients will be generated during the embedding procedures, so it is easy to reconstruct $B = \{b_1, b_2, \cdots, b_N\}$.

The embedded data can be easily extracted using (3) and the original block $b_i(u,v)$ is restored by (4).

$$d = \begin{cases} 0, & \text{if } |b_i'| = 1 \\ 1, & \text{if } |b_i'| = 2 \end{cases} \tag{3}$$

$$b_i = \begin{cases} \text{sign}(b_i'), & \text{if } 1 \le |b_i'| \le 2 \\ b_i' - \text{sign}(b_i'), & \text{if } |b_i'| \ge 3 \end{cases} \tag{4}$$

However, the distortion caused by data embedding is not just related to the number of zero AC coefficients, embedding secret data into two blocks with the same number of zero AC coefficients may result in different distortions. So the distribution of the AC coefficients must be taken into consideration.

B. Hou et al.'s Method

To solve the aforementioned problem, Hou *et al.* [9] improved the way to select the ± 1 AC coefficients, which is not only related to the number of zero AC coefficients, but also related to the distribution of the AC coefficients. Secret data is preferentially embedded into the nonzero coefficients with the frequencies yielding less distortion.

In this method [9], the quantization table is also taken into consideration. Firstly, we calculate the average distortion of each frequency in the quantized DCT blocks using (5).

$$\omega_{u,v} = \frac{\sum_{x=0}^{7}\sum_{y=0}^{7} \Delta f_{x,y}^2}{64} \tag{5}$$

where (u,v) represents the position of frequency, $\Delta f_{x,y}$ is calculated by IDCT and the quantization table. $\omega_{u,v}$ represents the weight of corresponding distortion in the spatial domain caused by modifying the AC coefficients.

$$D_{u,v} = (0.5 \cdot C_{u,v} + C_{\text{out}}) \times \omega_{u,v} \tag{6}$$

$D_{u,v}$ shows the total distortion of the frequency (u,v) in all blocks, $C_{u,v}$ is the number of AC coefficients valued ± 1, C_{out} is the number of AC coefficients whose absolute values are bigger than 1.

To handle both embedding capacity and visual distortion, we define $P_{u,v}$ as the reference of each frequency which is the basis for frequency sorting.

$$P_{u,v} = \frac{D_{u,v}}{C_{u,v}} \tag{7}$$

Then, we select the top K frequencies according to the ascending order of $P_{u,v}$, and compute the distortion of each block with only K frequencies. Finally, we select the blocks with small distortion to embed data.

The stage of calculating the average distortion of each frequency in the quantized DCT blocks is the highlight. Experimental results show that this method [9] has achieved better performance in both visual distortion and file size expansion.

C. Yin et al.'s Method

Huang *et al.*'s method [6] and Hou *et al.*'s method [9] both consider to reduce the embedding distortion and maximize the embedding capacity. However, as JPEG is a compress format, file size expansion after embedding data is also very important. Yin *et al.* [11] focused on combining all the factors to get the optimized combination by (8), which include three aspects: embedding capacity, distortion and file size expansion.

$$\begin{cases} \min\left(V * E^T\right) \\ \min\left(V * D^T\right) \end{cases} \quad \text{subject to} \quad C - V * R^T \le 0, \tag{8}$$

Here, $D = \{d_1, d_2, \cdots, d_k\}$, and d_i means the distortion of the ith block after embedding data. E is the file size expansion cost set, $E = \{e_1, e_2, \cdots, e_k\}$, also e_i means the ith block's file size expansion after embedding data. V is the decision variable, expressed in the form of $V = \{v_1, v_2, \cdots, v_k\}$, besides, $v_i \in \{0,1\}$, and if v_i equals 0, the ith block will not be used to embed data, and the ith block will be selected to embed data while v_i equals 1.

In addition, the $V * E^T$ represents the total file size expansion of the selected blocks. And $V * D^T$ represents the total distortion. Besides, C is the length of the embedded data and $V * R^T$ represents the total embedding capacity of the selected blocks, and $C - V * R^T \le 0$ is the constraint that the selected blocks must satisfy the payload.

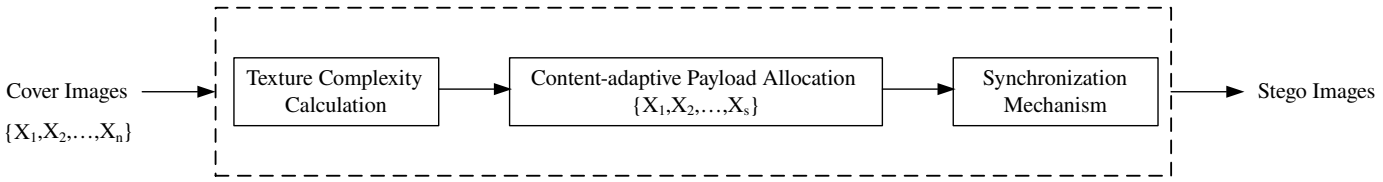

Fig. 1. Framework of the proposed undetectable JPEG image batch reversible data hiding method.

In conclusion, the above JPEG image reversible data hiding methods [6], [9], [11] exploit special manipulation on DCT coefficients for keeping the balance among visual distortion, file size expansion, and embedding capacity. The payload allocation strategy of these methods is essentially uniform payload allocation. Therefore, it is difficult for them to resist steganalytic detection [15]. Current JPEG image steganalytic features including 22510-dimensional ccJRM [16] and 7850-dimensional cfstar [17] can easily detect JPEG image reversible data hiding methods [6], [9], [11] with a high accuracy. Thus, JPEG image reversible data hiding methods cannot be directly applied in covert storage.

III. Proposed Undetectable JPEG Image Batch Reversible Data Hiding Method

To solve the problem that these state-of-the-art histogram shifting-based JPEG image reversible data hiding methods cannot resist steganalysis, the undetectable JPEG image batch reversible data hiding method is proposed in this paper. Firstly, the texture complexity of each JPEG image is modeled to determine the embedding order for cover images. Secondly, the content-adaptive payload allocation strategy is proposed to enhance the undetectability of JPEG image batch reversible data hiding. Thirdly, the synchronization mechanism is designed to guarantee the reversibility because the texture complexity may be modified after data embedding. The architecture of our proposed method is shown in Fig. 1.

A. Texture Complexity Calculation

Generally speaking, complex texture features are less vulnerable to steganalytic detection than simple texture features, indicating that more payload should be allocated in the region with complex texture [13]. Inspired by [20], we use kernels built from the one-dimensional low-pass wavelet decomposition filter $\mathbf{h}$ and the one-dimensional high-pass wavelet decomposition filter $\mathbf{g}$. In this case, the filters corresponding to two-dimensional LH, HL, and HH wavelet directional high-pass filters (L and H represent low-pass and high-pass filtered outputs) can be used to calculate residuals which coincide with the first-level undecimated wavelet LH, HL, and HH directional decomposition of cover images $\mathbf{X}_i$, $1 \leq i \leq n$. The three filters are depicted as follows.

$$\mathbf{K}^{(1)} = \mathbf{h} \cdot \mathbf{g}^{\mathrm{T}}, \mathbf{K}^{(2)} = \mathbf{g} \cdot \mathbf{h}^{\mathrm{T}}, \mathbf{K}^{(3)} = \mathbf{g} \cdot \mathbf{g}^{\mathrm{T}} \tag{9}$$

Given a pair of cover and stego images, $\mathbf{X}_i$ and $\mathbf{Y}_i$, we will denote their corresponding uvth wavelet coefficient in the kth subband of the first decomposition level as $W_{uv}^{(k)}(\mathbf{X}_i)$ and $W_{uv}^{(k)}(\mathbf{Y}_i)$, $k = 1, 2, 3$, $u \in \{1, \cdots, n_1\}, v \in \{1, \cdots, n_2\}$. The embedding cost is the sum of relative changes of all wavelet coefficients with respect to the cover image:

$$\omega_i \triangleq \sum_{k=1}^{3} \sum_{u=1}^{n_1} \sum_{v=1}^{n_2} \frac{\left| W_{uv}^{(k)}(\mathbf{X}_i) - W_{uv}^{(k)}(\mathbf{Y}_i) \right|}{\sigma + \left| W_{uv}^{(k)}(\mathbf{X}_i) \right|} \tag{10}$$

where $\sigma > 0$ is a constant stabilizing the numerical calculations.

The smaller ω_i indicates that the corresponding cover image $\mathbf{X}_i$ has more complex texture and higher embedding priority. Thus, ω_i can be modeled as the embedding cost of each image for batch reversible data hiding. We plot costs of 10000 images (chosen from BOSSbase [19]) as an example, which is showed in Fig. 2.

B. Content-adaptive Payload Allocation Strategy

In batch JPEG image reversible data hiding, the data hider wants to allocate m bits data among n JPEG images, and the payload allocation strategy greatly affects the undetectability [13]. Based on the texture complexity, the content-adaptive payload allocation strategy is proposed.

The content-adaptive payload allocation strategy intends to embed data for minimizing the total embedding costs of all cover images. During data embedding, the data hider iteratively chooses the image with the lowest embedding cost and embeds a portion of the data whose length equals the number of ± 1 AC coefficients in this image. It is assumed that a series of JPEG images are sorted by the embedding cost in ascending order. Then, the original embedding cost sequence $(\omega_1, \omega_2, \cdots, \omega_n)$ is sorted as $(\omega_{\sigma(1)}, \omega_{\sigma(2)}, \cdots, \omega_{\sigma(n)})$, where $\omega_{\sigma(1)} \leq \omega_{\sigma(2)} \leq \cdots \leq \omega_{\sigma(n)}$. Therefore, the allocated payload $m_{\sigma(i)}$ corresponding to each image is calculated by

$$\begin{cases} m_{\sigma(i)} = c_i, & \forall i \in \{1, \ldots, s-1\} \\ m_{\sigma(s)} = m - \sum_{i=1}^{s-1} m_{\sigma(s)} & \\ m_{\sigma(i)} = 0, & \forall i \in \{s+1, \ldots, n\} \end{cases} \tag{11}$$

where s denotes the number of selected images with lower embedding cost, which is calculated by (12). In (11), c_i represents the maximum embedding capacity of the ith image.

$$s = \arg \min_{1 \leq s \leq n} \sum_{i=1}^{s} \omega_i \quad \text{subject to} \quad \sum_{i=1}^{s} m_{\sigma(i)} \geq m. \tag{12}$$

Thus, the order of to-be-embedded images can be determined.

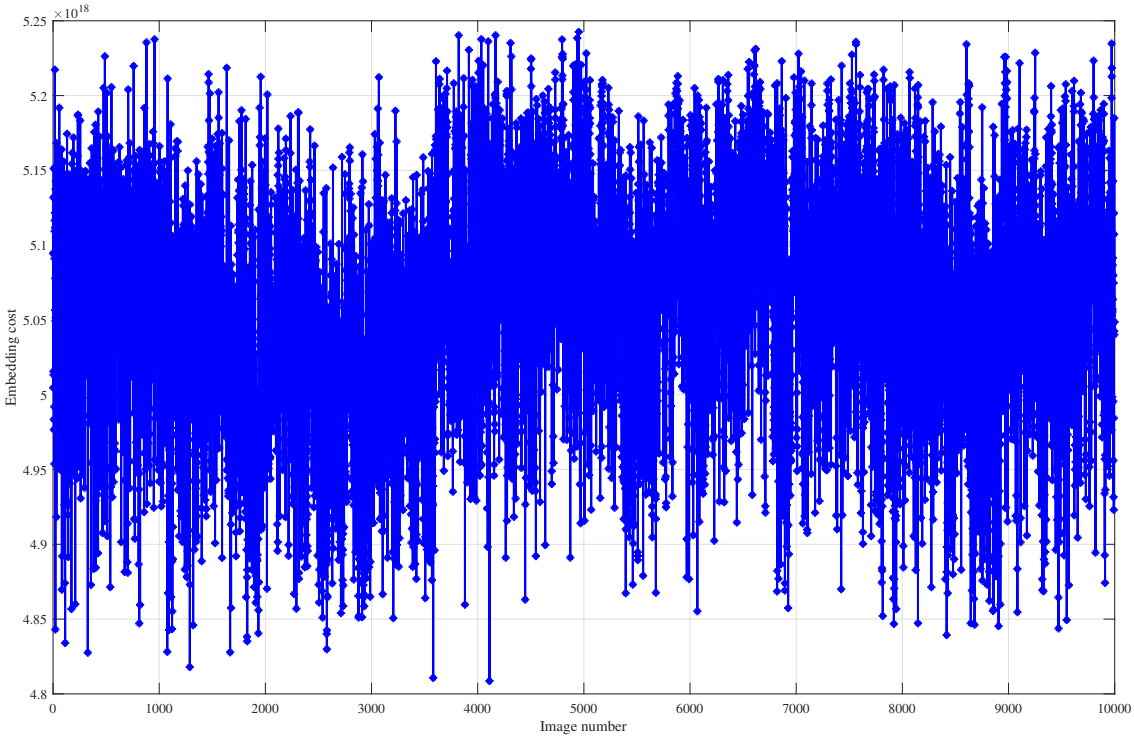

Fig. 2. Embedding costs of 10000 JPEG images.

C. Synchronization Mechanism

The texture complexity of each image may be modified after data embedding. In order to synchronize the texture complexity order before data extraction, we select one image $\mathbf{X}_h$ with least texture complexity (the largest embedding cost) as the header image for containing the sorted image index corresponding to $(\omega_{\sigma(1)}, \omega_{\sigma(2)}, \ldots, \omega_{\sigma(s)})$. Considering that the image index will not change a lot, we first calculate the difference of the sorted image index and the original image index, then RLE (Run Length Encoding) is used. The encoded information of the sorted image index will be embedded into the selected header image $\mathbf{X}_h$ using given JPEG image reversible data hiding method. To enhance the security, the encoded information should be encrypted before embedding. In our experiment, we choose RSA [18] as the encryption method. The details are beyond the scope of this paper and we will not discuss that here. Meanwhile, to prevent embedding data in the selected header image, we do not consider this header image $\mathbf{X}_h$ when performing the content-adaptive payload allocation strategy. Data extraction is the inverse process of data embedding.

IV. Experimental Results and Analysis

A. Experiment Setup

In this section, several comparative experiments are conducted to prove the security and undetectability of our proposed undetectable JPEG image batch reversible data hiding method. In the experiments, the content-adaptive payload allocation strategy is abbreviated as CPA. The BOSSbase [19] which consists of 10000 images is selected as the dataset. We set two payload allocation strategies which are uniform payload allocation strategy and our proposed content-adaptive payload allocation strategy. In the uniform payload allocation strategy, the relative payload is formulated as $\gamma = \frac{m}{n}$, where m represents the length of to-be-embedded data (in bits) and n is the total number of cover JPEG images. To generate stego images, we choose Huang *et al.*'s method [6], Hou *et al.*'s method [9], and Yin *et al.*'s method [11] as the seed algorithms where three different quality factors (QF) 60, 75, and 90 are used. The relative payload is abbreviated as embedded bits per image (in bpi).

We use ccJRM [16] to extract 22510-dimensional features and cfstar [17] to extract 7850-dimensional features for all cover-stego image pairs. Based on the extracted features, we utilize ensemble classifier to evaluate the undetectability of our proposed method. Ensemble classifier enables faster training and comparable detection accuracy compared with the classical support vector machines (SVM). A separate classifier is trained by half of cover-stego image features and the rest is used as the test set for each method and relative payload. The minimal total classification error rate under equal priors on the test set is defined as $P_{\mathrm{E}} = \min_{P_{\mathrm{FA}}} \frac{1}{2}(P_{\mathrm{FA}} + P_{\mathrm{MD}})$,

TABLE I
COMPARISONS OF AVERAGE CLASSIFICATION ERROR RATES $\overline{P_E}$ AT DIFFERENT RELATIVE PAYLOADS USING QF 60.

Feature	Strategy	Method	Relative payload (bpi)				
			2000	5000	8000	11000	14000
ccJRM	Uniform	Huang *et al.* [6]	0.1701 ± 0.0011	0.1697 ± 0.0005	0.1699 ± 0.0013	0.1701 ± 0.0010	0.1703 ± 0.0015
		Hou *et al.* [9]	0.1705 ± 0.0008	0.1703 ± 0.0015	0.1701 ± 0.0010	0.1703 ± 0.0008	0.1701 ± 0.0010
		Yin *et al.* [11]	0.1715 ± 0.0013	0.1710 ± 0.0016	0.1698 ± 0.0006	0.1702 ± 0.0006	0.1701 ± 0.0014
	CPA	Huang *et al.* [6]	0.4792 ± 0.0013	0.4467 ± 0.0009	0.4000 ± 0.0011	0.3544 ± 0.0013	0.2972 ± 0.0011
		Hou *et al.* [9]	0.4787 ± 0.0009	0.4474 ± 0.0005	0.3999 ± 0.0006	0.3540 ± 0.0005	0.2977 ± 0.0013
		Yin *et al.* [11]	0.4787 ± 0.0011	0.4472 ± 0.0014	0.3996 ± 0.0011	0.3542 ± 0.0010	0.2980 ± 0.0012
cfstar	Uniform	Huang *et al.* [6]	0.1744 ± 0.0028	0.1712 ± 0.0022	0.1710 ± 0.0014	0.1705 ± 0.0017	0.1704 ± 0.0005
		Hou *et al.* [9]	0.1752 ± 0.0012	0.1704 ± 0.0011	0.1707 ± 0.0009	0.1702 ± 0.0008	0.1705 ± 0.0014
		Yin *et al.* [11]	0.1723 ± 0.0014	0.1711 ± 0.0012	0.1707 ± 0.0015	0.1702 ± 0.0004	0.1701 ± 0.0014
	CPA	Huang *et al.* [6]	0.4797 ± 0.0018	0.4477 ± 0.0012	0.4007 ± 0.0009	0.3547 ± 0.0013	0.2981 ± 0.0012
		Hou *et al.* [9]	0.4798 ± 0.0029	0.4472 ± 0.0009	0.4008 ± 0.0009	0.3544 ± 0.0005	0.2979 ± 0.0014
		Yin *et al.* [11]	0.4797 ± 0.0012	0.4478 ± 0.0015	0.4009 ± 0.0009	0.3540 ± 0.0009	0.2974 ± 0.0013

TABLE II
COMPARISONS OF AVERAGE CLASSIFICATION ERROR RATES $\overline{P_E}$ AT DIFFERENT RELATIVE PAYLOADS USING QF 75.

Feature	Strategy	Method	Relative payload (bpi)				
			2000	6000	10000	14000	18000
ccJRM	Uniform	Huang *et al.* [6]	0.1615 ± 0.0014	0.1617 ± 0.0013	0.1611 ± 0.0003	0.1608 ± 0.0008	0.1614 ± 0.0011
		Hou *et al.* [9]	0.1628 ± 0.0015	0.1614 ± 0.0013	0.1607 ± 0.0008	0.1612 ± 0.0004	0.1610 ± 0.0012
		Yin *et al.* [11]	0.1613 ± 0.0005	0.1610 ± 0.0008	0.1609 ± 0.0007	0.1610 ± 0.0007	0.1611 ± 0.0012
	CPA	Huang *et al.* [6]	0.4837 ± 0.0013	0.4455 ± 0.0014	0.3954 ± 0.0008	0.3383 ± 0.0011	0.2685 ± 0.0010
		Hou *et al.* [9]	0.4841 ± 0.0011	0.4434 ± 0.0008	0.3944 ± 0.0010	0.3380 ± 0.0009	0.2686 ± 0.0015
		Yin *et al.* [11]	0.4834 ± 0.0013	0.4440 ± 0.0011	0.3947 ± 0.0007	0.3384 ± 0.0015	0.2679 ± 0.0012
cfstar	Uniform	Huang *et al.* [6]	0.1658 ± 0.0013	0.1624 ± 0.0024	0.1617 ± 0.0008	0.1620 ± 0.0019	0.1616 ± 0.0022
		Hou *et al.* [9]	0.1663 ± 0.0015	0.1624 ± 0.0016	0.1622 ± 0.0011	0.1614 ± 0.0013	0.1611 ± 0.0011
		Yin *et al.* [11]	0.1644 ± 0.0010	0.1623 ± 0.0009	0.1614 ± 0.0014	0.1607 ± 0.0007	0.1609 ± 0.0012
	CPA	Huang *et al.* [6]	0.4840 ± 0.0009	0.4442 ± 0.0010	0.3955 ± 0.0007	0.3379 ± 0.0007	0.2683 ± 0.0011
		Hou *et al.* [9]	0.4844 ± 0.0015	0.4441 ± 0.0007	0.3950 ± 0.0005	0.3381 ± 0.0011	0.2686 ± 0.0012
		Yin *et al.* [11]	0.4849 ± 0.0010	0.4441 ± 0.0006	0.3953 ± 0.0012	0.3380 ± 0.0008	0.2686 ± 0.0013

TABLE III
COMPARISONS OF AVERAGE CLASSIFICATION ERROR RATES $\overline{P_E}$ AT DIFFERENT RELATIVE PAYLOADS USING QF 90.

Feature	Strategy	Method	Relative payload (bpi)				
			2000	10000	18000	26000	30000
ccJRM	Uniform	Huang *et al.* [6]	0.1884 ± 0.0012	0.1873 ± 0.0013	0.1869 ± 0.0007	0.1876 ± 0.0015	0.1873 ± 0.0013
		Hou *et al.* [9]	0.1899 ± 0.0018	0.1878 ± 0.0013	0.1878 ± 0.0012	0.1868 ± 0.0004	0.1871 ± 0.0009
		Yin *et al.* [11]	0.1888 ± 0.0013	0.1875 ± 0.0014	0.1872 ± 0.0011	0.1873 ± 0.0013	0.1875 ± 0.0014
	CPA	Huang *et al.* [6]	0.4875 ± 0.0010	0.4341 ± 0.0007	0.3670 ± 0.0009	0.2900 ± 0.0007	0.2517 ± 0.0015
		Hou *et al.* [9]	0.4879 ± 0.0009	0.4340 ± 0.0013	0.3704 ± 0.0012	0.3040 ± 0.0016	0.2777 ± 0.0013
		Yin *et al.* [11]	0.4881 ± 0.0009	0.4343 ± 0.0008	0.3670 ± 0.0005	0.2899 ± 0.0012	0.2520 ± 0.0018
cfstar	Uniform	Huang *et al.* [6]	0.1969 ± 0.0049	0.1880 ± 0.0011	0.1878 ± 0.0013	0.1878 ± 0.0013	0.1871 ± 0.0006
		Hou *et al.* [9]	0.1956 ± 0.0029	0.1872 ± 0.0006	0.1882 ± 0.0014	0.1874 ± 0.0011	0.1872 ± 0.0012
		Yin *et al.* [11]	0.1949 ± 0.0017	0.1880 ± 0.0012	0.1871 ± 0.0012	0.1871 ± 0.0007	0.1880 ± 0.0014
	CPA	Huang *et al.* [6]	0.4881 ± 0.0009	0.4345 ± 0.0012	0.3673 ± 0.0013	0.2903 ± 0.0013	0.2517 ± 0.0012
		Hou *et al.* [9]	0.4875 ± 0.0011	0.4343 ± 0.0007	0.3705 ± 0.0014	0.3030 ± 0.0000	0.2772 ± 0.0008
		Yin *et al.* [11]	0.4890 ± 0.0014	0.4341 ± 0.0011	0.3677 ± 0.0011	0.2907 ± 0.0012	0.2525 ± 0.0011

P_{FA} is the false alarm rate and P_{MD} is the missed detection rate. The ultimate undetectability is qualified by the average classification error rate $\overline{P_{\text{E}}}$ which is the mean value of P_{E} over ten random splits of the test set, and large $\overline{P_{\text{E}}}$ means stronger undetectability. $\overline{P_{\text{E}}}$ is reported in the form of mean and standard variance for reflecting statistical significance. It should be noted that $P_{\text{E}} = \frac{1}{2}$ means perfect undetectability.

B. Experiment Steps

To perform JPEG image batch reversible data hiding, following steps should be performed when payload allocation strategy is given.

- Calculate the embedding cost ω_i using (9) and (10) and obtain the embedding cost sequence $\omega_i, 1 \leq i \leq n$.
- Sort the embedding cost sequence $\omega_i, 1 \leq i \leq n$ in ascending order and select the header image $\mathbf{X}_h$.
- Calculate the data length corresponding to each image using the given payload allocation strategy and complete m bits data hiding in cover images excluding the header image $\mathbf{X}_h$.

C. Undetectability Comparison

The comparisons of average classification error rates $\overline{P_{\text{E}}}$ at different relative payloads are summarized in Table I, Table II, and Table III, where QF 60, QF 75, and QF 90 are used respectively, and ensemble classifiers are chosen for steganalytic detection. It can be seen that the $\overline{P_{\text{E}}}$ decreases with the increase of the relative payload and QF for our CPA method. Moreover, the undetectability is improved after employing our proposed payload allocation strategy CPA for each JPEG image reversible data hiding method. Specifically, at relative payload 2000 bpi, the $\overline{P_{\text{E}}}$ using our proposed payload allocation strategy CPA outperforms that using the uniform payload allocation by 0.3091 for Huang *et al.*'s method [6].

The state-of-the-art JPEG image steganalysis aims to extract image-level features which represent the statistical characteristics of DCT coefficients. In uniform payload allocation strategy, each stego image contains the same relative payload. As a result, conspicuous data embedding traces can be exploited by attackers. Since data can be embedded into the images with the minimal embedding cost sum and the sufficient embedding capacity using our proposed payload allocation strategy CPA, the statistical characteristics of more DCT coefficient are preserved. Besides, although it is inevitable that calculating the embedding costs will bring extra computation, the increase in time is acceptable.

From the average PSNR in Table IV, Table V, and Table VI, we can see clearly that our proposed CPA strategy will just slightly affect the overall image quality compared with the uniform payload allocation strategy. Specifically, the average PSNR keeps almost the same for our CPA method under different relative payloads and QF values.

TABLE IV
COMPARISONS OF AVERAGE PSNR AT DIFFERENT RELATIVE PAYLOADS USING QF 60.

Strategy	Method	Relative payload (bpi)				
		2000	5000	8000	11000	14000
Uniform	Huang *et al.* [6]	36.9910	36.6965	36.3641	35.9885	35.5542
	Hou *et al.* [9]	37.0005	36.7375	36.4217	36.0563	35.6107
	Yin *et al.* [11]	37.0377	36.8067	36.5067	36.1376	35.6787
CPA	Huang *et al.* [6]	36.9806	36.7030	36.3674	36.0051	35.5710
	Hou *et al.* [9]	36.9806	36.7028	36.3675	36.0046	35.5716
	Yin *et al.* [11]	36.9806	36.7032	36.3677	36.0056	35.5736

TABLE V
COMPARISONS OF AVERAGE PSNR AT DIFFERENT RELATIVE PAYLOADS USING QF 75.

Strategy	Method	Relative payload (bpi)				
		2000	6000	10000	14000	18000
Uniform	Huang *et al.* [6]	38.6990	38.3936	38.0177	37.5651	37.0081
	Hou *et al.* [9]	38.7065	38.4333	38.0741	37.6267	37.0583
	Yin *et al.* [11]	38.7309	38.4903	38.1464	37.6990	37.1176
CPA	Huang *et al.* [6]	38.6515	38.2863	37.8639	37.4004	36.8709
	Hou *et al.* [9]	38.6515	38.2859	37.8634	37.3995	36.8700
	Yin *et al.* [11]	38.6515	38.2857	37.8631	37.3997	36.8706

TABLE VI
COMPARISONS OF AVERAGE PSNR AT DIFFERENT RELATIVE PAYLOADS USING QF 90.

Strategy	Method	Relative payload (bpi)				
		2000	10000	18000	26000	30000
Uniform	Huang *et al.* [6]	42.5347	42.1136	41.4598	40.6776	40.2244
	Hou *et al.* [9]	42.5396	42.1443	41.5009	40.7027	40.2400
	Yin *et al.* [11]	42.5485	42.1847	41.5621	40.7672	40.2591
CPA	Huang *et al.* [6]	42.4448	41.8165	41.0983	40.3528	39.9740
	Hou *et al.* [9]	42.4448	41.8166	41.1192	40.5110	40.2322
	Yin *et al.* [11]	42.4452	41.8166	41.0978	40.3511	39.9728

V. CONCLUSION AND FUTURE WORK

Batch image data hiding attracts increasing attention in recent years because it provides an efficient way to achieve covert storage in clouds. Reversible data hiding which can completely restore the original cover after data extraction brings about novel advantages for JPEG image-based covert storage. In this paper, the undetectable JPEG image batch reversible data hiding method is proposed. Firstly, the texture complexity of each JPEG image is modeled to determine the embedding order of cover images. Secondly, the content-adaptive payload allocation strategy is proposed to enhance the undetectability of JPEG image batch reversible data hiding. Thirdly, the synchronization mechanism is designed to guarantee the reversibility because the texture complexity may be modified after data embedding. Experimental results demonstrate the superiority of this proposed method compared with the state-of-the-art related methods.

For further study, the adversarial mechanism based on complicated steganalytic features deserves investigation for efficiently detecting JPEG image batch reversible data hiding.

ACKNOWLEDGMENTS

This work was supported in part by the National Key Research and Development Program of China under Grant 2018YFB0804102, in part by the National Natural Science Foundation of China under Grant 61802357, and in part by the Fundamental Research Funds for the Central Universities under Grant WK3480000009.

REFERENCES

[1] J. Fridrich, M. Goljan, and R. Du, "Lossless data embedding for all image formats," in *Proc. SPIE - The International Society for Optical Engineering*, vol. 4675, pp. 572–583, Apr. 2002.

[2] J. Tian, "Reversible data embedding using a difference expansion," *IEEE Trans. Circuits Syst. Video Technol.*, vol. 13, no. 8, pp. 890–896, Aug. 2003.

[3] Z. Ni, Y.-Q. Shi , N. Ansari, and W. Su, "Reversible data hiding," *IEEE Trans. Circuits Syst. Video Technol.*, vol. 16, no. 3, pp. 354–362, Mar. 2006.

[4] X. Li, B. Li, B. Yang, and T. Zeng, "General framework to histogram-shifting-based reversible data hiding," *IEEE Trans. Image Process.*, vol. 22, no. 6, pp. 2181–2191, Jun. 2013.

[5] B. Ou, X. Li, Y. Zhao, R. Ni, and Y.-Q. Shi, "Pairwise prediction-error expansion for efficient reversible data hiding," *IEEE Trans. Image Process.*, vol. 22, no. 12, pp. 5010–5021, Dec. 2013.

[6] F. Huang, X. Qu, H.J. Kim, and J. Huang, "Reversible data hiding in JPEG images," *IEEE Trans. Circuits Syst. Video Technol.*, vol. 26, no. 9, pp. 1610–1621, Sep. 2016.

[7] N. Li and F. Huang, "Reversible data hiding for JPEG images based on pairwise nonzero AC coefficient expansion," *Signal Process.*, vol. 171, Jun. 2020, Art. no. 107476.

[8] F.T. Wedaj, S. Kim, H.J. Kim, and F. Huang, "Improved reversible data hiding in JPEG images based on new coefficient selection strategy," *Eurasip J. Image Video Process.*, vol. 2017, no. 1, pp. 1–11, Dec. 2017.

[9] D. Hou, H. Wang, W. Zhang, and N. Yu, "Reversible data hiding in JPEG image based on DCT frequency and block selection," *Signal Process.*, vol. 148, pp. 41–47, Jul. 2018.

[10] J. He, X. Pan, H.-T. Wu, and S. Tang, "Improved block ordering and frequency selection for reversible data hiding in JPEG images," *Signal Process.*, vol. 175, Oct. 2020, Art. no. 107647.

[11] Z. Yin, Y. Ji, and B. Luo, "Reversible Data Hiding in JPEG Images With Multi-Objective Optimization," *IEEE Trans. Circuits Syst. Video Technol.*, vol. 30, no. 8, pp. 2343–2352, Aug. 2020.

[12] Facebook by the Numbers [Online].
Available: http://omnicoreagency.com/facebook-statistics/

[13] A.D. Ker, P. Bas, R. Bohme, R. Cogranne, S. Craver, T. Filler, J. Fridrich, and T. Pevny, "Moving steganography and steganalysis from the laboratory into the real world," in *Proc. 1st ACM Workshop Inf. Hiding Multimedia Secur. (IH and MMSec)*, Jun. 2013, pp. 45–58.

[14] D.M. Thodi and J.J. Rodriguez, "Expansion embedding techniques for reversible watermarking," *IEEE Trans. Image Process.*, vol. 16, no. 3, pp. 721–730, Mar. 2007.

[15] A.D. Ker, "A capacity result for batch steganography," *IEEE Signal Process. Letters.*, vol. 14, no. 8, pp. 525–528, Aug. 2007.

[16] J. Kodovsky and J. Fridrich, "Steganalysis of JPEG images using rich models," in *Proc. SPIE - The International Society for Optical Engineering.*, vol. 8303, Jan. 2012, Art. no. 83030A.

[17] J. Kodovsky, J. Fridrich, and V. Holub, "Ensemble classifiers for steganalysis of digital media," *IEEE Trans. Inf. Forensics Security.*, vol. 7, no. 2, pp. 432–444, Apr. 2012.

[18] R.L. Rivest, A. Shamir, and L. Adleman, "A Method for Obtaining Digital Signatures and Public-Key Cryptosystems," *Communications of the ACM*, vol. 21, no. 2, pp. 1200–126, Feb. 1978.

[19] BOSSbase [Online].
Available: http://dde.binghamton.edu/download/

[20] V. Holub, J. Fridrich, and T. Denemark, "Universal distortion function for steganography in an arbitrary domain," *Eurasip J. Info. Security.*, Jan. 2014, Art. no. 1.